Published in final edited form as:
*Am J Ophthalmol*. 2010 May ; 149(5): 817–25.e1. doi:10.1016/j.ajo.2009.12.007.

# Structure-Function Correlations using Scanning Laser Polarimetry in Primary Angle-Closure Glaucoma and Primary Open Angle Glaucoma

**Pei-Jung Lee**[1], **Catherine Jui-Ling. Liu**[1,2], **Robert Wojciechowski**[3], **Joan E. Bailey-Wilson**[3], and **Ching-Yu Cheng**[1,2,3,4]

[1]Department of Ophthalmology, Taipei Veterans General Hospital, Taipei, Taiwan [2]National Yang Ming University School of Medicine, Taipei, Taiwan [3]Inherited Disease Research Branch, National Human Genome Research Institute, National Institutes of Health, Baltimore, Maryland [4]Department of Epidemiology, Johns Hopkins University Bloomberg School of Public Health, Baltimore, Maryland

## Abstract

**Purpose—**To assess the correlations between retinal nerve fiber layer (RNFL) thickness measured with scanning laser polarimetry (SLP) and visual field (VF) sensitivity in primary open angle glaucoma (POAG) and primary angle-closure glaucoma (PACG).

**Design—**Prospective, comparative, observational cases series

**Methods—**Fifty patients with POAG and 56 with PACG were examined using SLP with variable corneal compensation (GDx VCC) and Humphrey VF analyzer between August 2005 and July 2006 at Taipei Veterans General Hospital. Correlations between RNFL thickness and VF sensitivity, expressed as mean sensitivity (MS) in both decibel (dB) and 1/Lambert (L) scales, were estimated by Spearman's rank correlation coefficient ($r_s$) and multivariate median regression models (pseudo $R^2$). The correlations were determined globally and for six RNFL sectors and their corresponding VF regions.

**Results—**The correlation between RNFL thickness and MS (in dB) was weaker in the PACG group ($r_s$ = 0.38, *P* = 0.004, pseudo $R^2$ = 0.17) than in the POAG group ($r_s$ = 0.51, *P* <0.001, pseudo $R^2$ = 0.31), but the difference in the magnitude of correlation was not significant (*P* = 0.42).With Bonferroni correction, the structure-function correlation was significant in the superotemporal ($r_s$ = 0.62), superonasal ($r_s$ = 0.56), inferonasal ($r_s$ = 0.53), and inferotemporal ($r_s$ = 0.50) sectors in the POAG group (all *P* <0.001), while it was significant only in the superotemporal ($r_s$ = 0.53) and inferotemporal ($r_s$ = 0.48) sectors in the PACG group (both *P* <0.001). The results were similar when MS was expressed as 1/L scale.

Address for reprints and correspondence to: Ching-Yu Cheng, MD, MPH, Department of Ophthalmology, Taipei Veterans General Hospital, Taipei, Taiwan, 201 Shih-Pai Rd Section 2, Taipei, Taiwan, Phone number: +886-2-28758325, cycheng@jhsph.edu.

Financial Disclosures: none

Contributions of Authors: Design and conduct of the study (CJL, CYC); Data collection (PJL, CJL); Analysis and interpretation of the data (PJL, CJL, CYC); Statistical expertise (RW, JEB, CYC); Preparation of the manuscript (PJL); Revision of the article (CJL, RW, JEB, CYC); Final approval of the manuscript (CJL, CYC)

Statement about Conformity with Author Information: All persons gave their informed consent prior to being included in the study. This study protocol followed the Declaration of Helsinki tenets and was approved by the Institutional Review Board, Taipei Veterans General Hospital, Taipei, Taiwan.

Other Acknowledgments: none

**Conclusions—**Both POAG and PACG eyes had moderate structure-function correlations using SLP. Compared to eyes with POAG, fewer RNFL sectors have significant structure-function correlations in eyes with PACG.

Glaucoma is a progressive optic neuropathy characterized by loss of retinal ganglion cells and their axons, which results in thinning of the retinal nerve fiber layer (RNFL) and a reduction of visual field (VF) sensitivity. Both structural and functional losses provide important information in the diagnosis and evaluation of glaucoma. Structural loss is assessed clinically by evaluating the cup-to-disc ratio, neuroretinal rim dimensions and RNFL thickness. Among these, RNFL atrophy may precede the changes in optic disc.[1] New imaging technologies provide objective and quantitative measurements of RNFL thickness. Several studies have reported structure-function associations in glaucoma between VF sensitivity and RNFL thickness using a variety of imaging technology, including scanning laser polarimetry (SLP), confocal scanning laser ophthalmoscopy and optical coherence tomography (OCT).[2-6] The strength of associations are generally moderate with a coefficient of determination ranging from 0.11 – 0.62, depending on perimetry scale, RNFL measuring instruments and the patient characteristics.

The pathophysiology of primary open angle glaucoma (POAG) includes an interplay of multiple factors such as reduced perfusion to the optic nerve, abnormalities of axonal or ganglion cell metabolism, and disorders of the extracellular matrix of the lamina cribrosa. The current classification scheme defines primary angle-closure glaucoma (PACG) as an eye with glaucomatous optic neuropathy and VF defect similar to those in POAG and an occludable drainage angle.[7] Most cases of PACG are asymptomatic and chronic. Chronic PACG may develop after the resolution or precede an acute attack of angle closure.[8, 9] Unlike POAG, in which high intraocular pressure (IOP) is just one of several risk factors, the pathogenetic mechanism of optic neuropathy in PACG is primarily IOP-dependent secondary to a crowded anterior segment.[10] Evidence has shown that the pattern of VF defect and the relationship of peripapillary atrophy to the structural and functional optic disc changes are different between POAG and PACG, suggesting differences in the pathophysiology of optic nerve damage.[11, 12]

Previous studies of structure-function correlations included mostly participants with POAG.[4, 6, 13] In light of the concept that the pathophysiological characteristics in PACG may differ from those in POAG, we suggest a hypothesis that the structure-function correlations differ between these two forms of glaucoma. If differences exist, it would be important to take them into account while making the diagnosis and detecting disease progression. Furthermore, such differences might shed light on the underlying pathophysiology of the two disease entities. In this prospective observational case series, we aimed to compare the structure-function relationship between patients with controlled POAG and PACG by using SLP with variable corneal compensation (GDx VCC) and automated perimetry.

## Patients & Methods

### Subjects

One hundred sixty-five PACG patients and 150 high-tension POAG patients who fulfilled the clinical inclusion criteria were recruited consecutively and prospectively by one glaucoma specialist (CJL) between August 2005 and July 2006 at Taipei Veterans General Hospital. Among them, 23 PACG and 29 POAG patients were excluded because of unreliable VF data, and additional 86 PACG and 71 POAG patients were excluded due to unqualified SLP image. This left a total of 56 PACG and 50 POAG eligible subjects in the present study. All participants underwent a comprehensive ophthalmologic evaluation, including refraction, best corrected visual acuity (BCVA), slit lamp biomicroscopy, tonometry, gonioscopy, SLP with variable

corneal compensation, and achromatic automated perimetry. In addition, the optic discs were assessed by dilated ophthalmoscopy with a 78 D lens and optic disc photography.

The diagnosis of POAG was based on normal open angles, baseline, untreated IOP ≥21 mmHg, and reproducible nerve fiber bundle VF defects in at least 2 consecutive field tests that corresponded to the glaucomatous optic disc changes (diffuse or local rim thinning, notching, and excavation). The diagnosis of PACG was based on the same criteria as POAG except that the anterior chamber angle was occludable before laser iridotomy with the posterior trabecular meshwork visible for less than 90° of the angle circumference. Inclusion criteria were BCVA of 20/40 or better, cylinder refraction within ±3.0 D, controlled IOP (<24 mmHg for at least 6 months) at enrollment, and reliable VF test and qualified SLP imaging obtained within a 3-month interval. Patients with glaucoma secondary to medication or other ocular abnormalities, retinal diseases or other neurological disease that may cause VF defects, or having received laser or incisional ocular surgery within three months were excluded. This study did not include the subgroup of normal tension glaucoma, and we aimed at comparing the structure-function correlations between patients with high pressure POAG and PACG.

## Automated Perimetry

Visual field tests were performed with 24-2 Swedish Interactive Threshold Algorithm (SITA) standard of the Humphrey Field Analyzer 750 (Carl Zeiss Meditec, Inc., Dublin, CA). Reliability criteria for VF results were fixation loss ≤33%, false positive response ≤20%, and false negative response ≤20%.[14-16] These reliability criteria that were adopted for the Full Threshold strategy might not be strict enough for the SITA standard, but to the best of our knowledge no published criteria existed for the SITA standard. A glaucomatous VF defect was defined as a glaucoma hemifield test result outside normal limits, a pattern standard deviation (PSD) outside 95% of age-specific normal limits, or a mean deviation (MD) outside 95% of age-specific normal limits which is not attributable to other causes in an eye with a BCVA better than 20/25. The VF results were graded based on the scoring system adopted by the Advanced Glaucoma Intervention Study (AGIS).[17] The eye with the lower AGIS score was selected if both eyes of one patient fulfilled all the inclusion criteria and none of the exclusion criteria. The AGIS scoring method requires larger depressions for peripheral locations to be considered defective than that for central locations, and it takes the distribution of retinal nerve fibers into consideration. Therefore, variations in AGIS score may reflect differences in the severity of glaucomatous optic neuropathy better than variations in MD.

Visual field sensitivity was expressed in two ways: exact visual sensitivity in decibel units (dB, raw thresholds) and 1/Lambert (L) scale. At each test point, the differential light sensitivity is measured in dB as $10 \times \log_{10} [L_{max}/ (L_t-L_b)]$, where $L_{max}$ is the maximal stimulus luminance, $L_t$ is the stimulus luminance at threshold and $L_b$ is the stimulus luminance at background. Thus the 1/L scale is proportional to $10^{dB/10}$, for simplicity. We used the 1/L scale to avoid the log transformation within the decibel scale.

The mean sensitivity (MS) was obtained by averaging thresholds at each of the 52 test points to determine the global structure-function association. Garway-Heath et al. mapped the VF test points corresponding to six sectors of optic disc (Figure 1).[18] The VF was divided into six sectors as defined by Reus et al.[2], which were based on Garway-Heath's optic disc-visual field map. Averaged thresholds from each sector were calculated for further structure-function comparisons of the six corresponding sectors.

## Scanning Laser Polarimetry

The RNFL was evaluated with the GDx VCC system, software version 5.5.0 (Laser Diagnostic technologies, Inc., San Diego, CA) in patients with eyes undilated. The GDx VCC measures

the summed retardation of a laser light beam that double passes the RNFL, and its working principles have been described in detail elsewhere.[19] Images were included only if they were well-focused, evenly-illuminated, and with good centering. Scan images with a quality score <7, with atypical birefringence pattern, or with vitreous degeneration affecting the ellipse and the peripapillary circle were excluded. An atypical birefringence pattern is defined as peripapillary high retardation arranged circumferentially or in a spokelike pattern, or splotchy areas of high retardation nasally and temporally.[20] A medium-sized measurement circle, rather than a small-sized circle, centered on the optic disc with an inner diameter of 3.2 mm and an outer diameter of 4.0 mm was chosen for RNFL assessment because of higher prevalence of peripapillary atrophy and greater peripapillary atrophy-to-disc area ratio in POAG compared to those in PACG.[12] The edge of the optic disc was automatically defined by the GDx machine as the inner margin of the peripapillary scleral ring, which was checked by a trained examiner and manually adjusted if inaccurately defined by the GDx algorithm. The resulting horizontal and vertical disc diameters as shown on the GDx printout were used for analysis.

The GDx VCC standard parameters, including temporal–superior–nasal–inferior–temporal (TSNIT) average, TSNIT standard deviation (SD), and the nerve fiber index (NFI) were collected. The TSNIT average is equivalent to the average RNFL thickness along the measurement circle, and the TSNIT SD is the standard deviation of RNFL measurements along the circle and it captures the peak to trough difference in the RNFL thickness. The NFI is calculated using a support vector machine algorithm based on several RNFL measurements to optimally differentiate glaucoma from normal. The higher the NFI, the greater the likelihood the patient has glaucoma. The GDx VCC device also processed the RNFL thickness measurements for 64 regions along the circumpapillary measurement circle. The 64 peripapillay regions in the GDx VCC retardation image and the 52 VF test points were subsequently grouped into six corresponding sectors based on the previously published optic disc-visual field map[18] and named after the position of the sector in the GDx VCC image relative to the disc. Because of the fixed exported sectors in the GDx VCC measurements, the six optic nerve head sectors were modified slightly but still consistent with their relationship to the VF testing points. The six modified optic nerve head sectors were: temporal (T, 310-39°), superotemporal (ST, 40-79°), superonasal (SN, 80-118°), nasal (N, 119-226°), inferonasal (IN, 227-271°) and inferotemporal (IT, 272-309°).

## Statistical Analysis

Statistical analyses were performed with Stata statistical software (Stata Corp, College Station, TX). Because of the non-normal distribution of the VF sensitivity data, Spearman's rank correlation coefficient ($r_s$) was used to determine the correlation between VF MS and RNFL thickness for global measurements and for each of the six sectors. Bonferroni correction was used to control the overall type I error rate at 0.05 to account for multiple testing across sectors; that is, a *P* value <0.0083 (0.05/6) was considered statistically significant for each sector. The differences in the correlations between the two groups were tested using Fisher's r z transformation.

Multivariate median regression analysis, with VF sensitivity as the dependent variable, RNFL thickness as the independent variable, and age, sex, axial length, optic disc diameters (as shown on the GDx VCC printout) as covariates was subsequently performed in the whole field and in each of the six sectors. We used median regression, instead of regular (i.e., mean-squared error loss) linear regression, to account for the non-normality of our data.[21] The coefficient of determination in the median regression, pseudo $R^2$, was calculated to represent the proportion of variability in VF sensitivity that can be explained by a given regression model.

## Results

A total of 50 patients with POAG and 56 with PACG were recruited in the present analysis and all were of Chinese ethnic background. The characteristics of the two groups are summarized in Table 1. Of the 106 included patients, 17 had received cataract surgery and 29 had undergone trabeculectomy more than 3 months prior to being enrolled into this study. For these patients, the VF and GDx data obtained at least 3 months after surgery were analyzed in this study. All the PACG patients had received laser iridotomy. Among the 56 PACG eyes, 2 had a history of acute angle-closure attack that occurred at least 5 years before and 6 had a plateau iris configuration. In general, the POAG patients were younger, tended to be more myopic and had longer axial lengths and smaller disc diameters, compared to PACG patients (all $P$ <0.001). Both the three GDx VCC standard parameters (TSNIT average, TSNIT SD and NFI) and VF global index (MS, MD, and PSD) were comparable between the two groups (all $P$ >0.05). Comparing the sectoral RNFL thickness with adjustments of age, sex and axial length, there was no significant difference between POAG and PACG subjects (all $P$ > 0.05, data not shown). The mean sensitivity in each of the six sectors was also comparable between the two groups after multivariate analysis (all $P$ > 0.05, data not shown).

### Global Structure-Function Associations

Figure 2 shows a scatter plot of VF MS versus average RNFL thickness (TSNIT average). There were significant global correlations between TSNIT average and VF MS in both POAG ($P$ <0.001) and PACG ($P$ = 0.004) groups, but the correlation was weaker in the PACG group ($r_s$ = 0.38) than that in the POAG group ($r_s$ = 0.51) (Table 2). The multivariate regression model also accounted for less variability of VF sensitivity data in the PACG group (pseudo $R^2$ = 0.17) than in the POAG group (pseudo $R^2$ = 0.31). Although the magnitude of global correlation was weaker in PACG than in POAG, the difference did not reach statistically significant ($P$ = 0.42). Similarly, a trend of weaker global correlation in the PACG group was observed when VF sensitivity was expressed as 1/L scale (Table 3), but again the difference in the strength of correlation was not significant ($P$ = 0.58).

### Sector-Specific Structure-Function Associations

When investigating structure-function correlations in the six corresponding sectors, the correlation coefficients were significant in the ST, SN, IT and IN sectors (all $P$ <0.001) in the POAG group when VF sensitivity was expressed in dB (Table 2) or in 1/L scales (Table 3). In the PACG group, the correlations were significant in the ST and IT sectors (both $P$ <0.001). Figure 3 presents the scatter plots of VF sensitivity (in dB scale) versus RNFL thickness for the ST, SN, IT and IN sectors. Structure-function correlations were strongest in the ST sector in both measurement scales in both groups. There was no statistically significant correlation between structure and function in the temporal and nasal sectors in either group.

In order to further account for the possible effect of age differences, we removed the 25% youngest patients from the POAG group and the 25% oldest from the PACG group. This reduced the sample size, leaving 37 patients in the POAG group and 43 in the PACG group, but enabled us to make comparisons between groups with similar age (POAG, 68.1 ± 12.7 years and PACG, 68.2 ± 8.4 years, $P$ =0.974). We found that the global correlation between TSNIT average and VF MS in the PACG group ($r_s$ = 0.24, $P$ = 0.125) was still weaker than that in the age-matched POAG group ($r_s$ = 0.46, $P$ = 0.005), but again, the difference in the magnitude of correlation was not statistically significant ($P$ = 0.28). Similarly, the POAG eyes had statistically significant structure-function correlations (all $P$ <0.0083) in the ST, SN, IT and IN sectors, while the PACG eyes had significant correlation only in the ST sector.

## Discussion

We have demonstrated a moderate correlation between the measurement of VF sensitivity using standard automated perimetry and the measurement of RNFL thickness, as assessed by GDx VCC, in both POAG and PACG patients. The global correlation between VF MS and TSNIT average was weaker, but not to a statistically significant extent, in PACG as compared to that in POAG. Besides, we found significant structure-function correlations in more sectors in POAG eyes than in PACG eyes. To our knowledge, this is the first comparative study of structure-function correlations using SLP for PACG versus POAG.

In the POAG group, significant structure-function correlations were found in the sectors of ST, SN, IT, and IN. However, only two sectors (ST and IT) out of six had significant structure-function correlation in the PACG group, which might have compromised the global correlation in this form of glaucoma. The exact reason for this disparity between the two groups is unclear. We speculated that this disparity may be, at least in part, related to the difference in axial length between groups. Recent studies comparing eye shape between emmetropic and myopic eyes showed that myopic eyes tended to be greater in all dimensions with a possible global expansion or a radial volume expansion.[22, 23] In contrast, a globe with a shorter axial length may have a steeper radius at the posterior pole of the globe. The GDx VCC laser light will pass through the RNFL at a slightly different angle between globes with a steeper and a flatter radius at the posterior pole. The RNFL measurement nasal to the disc may be particularly vulnerable to this variation because of its low magnitude and the fact that optic nerve enters the globe from the nasal side. The more tangential pathway of the laser light crossing through the nasal RNFL may decrease the accuracy of GDx VCC measurement and negatively affect the structure-function correlation.

Another possible reason for the observed disparity in structure-function correlations across sectors between POAG and PACG is different pathophysiological process of the two disease entities. In a study comparing the optic disc and VF alterations in 110 POAG patients and 36 PACG patients, Boland and associates found that, for a given level of VF sensitivity, the average RNFL thickness as measured by OCT was significantly greater in PACG than that in POAG, which held true even after controlling for VF mean deviation, Heidelberg Retina Tomograph disc area, and axial length.[24] Despite that they did not assess the difference by RNFL sectors, their findings suggest different structure-function relationships between these two forms of glaucoma. Evidence shows that microtubules in nerve fiber bundles are the major contributors for RNFL birefringence and microtubules are expected to disappear after the ganglion cells die.[25] It remains to be clarified whether the time lag between cell death and microtubules disappearance or other subcellular changes differ between POAG and PACG.

One concern is that the fewer sectors with significant structure-function correlations we noted in the PACG eyes might be caused simply by poorer SLP imaging quality in this group of older patients, resulting from denser media opacity or more eye movements. Mai et al. suggested GDx with enhanced corneal compensation (ECC) revealed stronger structure-function correlations than did GDx VCC because of higher signal-to-noise ratio in the GDx ECC.[26] However, these differences were no longer observed when only images with typical birefringence patterns were included for analysis.[26] In the present study, atypical scans were excluded and quality scores of the GDx VCC images were comparable between the two groups (POAG: 8.4 ± 0.6 vs. PACG: 8.3 ±0.7, $P > 0.05$). It is therefore unlikely that the difference in image quality between the two groups was a source of the observed differences in structure-function correlation.

Our findings that no significant structure-function association exist in either the temporal or nasal sector in each diagnostic group were consistent with previous studies.[2-4] The lack of

association in these sectors may be caused by several factors. One is that the RNFL birefringence varies with the position around the optic nerve head in human subjects,[27,28] and the fixed conversion factor used in the GDx VCC algorithm makes the calculation of RNFL thickness less accurate, particularly in the temporal and nasal sectors. Another reason is that the GDx VCC measurements are less accurate for thinner RNFL. Finally, a likely source of error in the estimates of association between the nasal peripapillary RNFL and its corresponding VF sector resides in the design of the VF test itself. Specifically, the temporal visual field is poorly sampled by the Humphrey Field Analyzer 24-2 algorithm, which results in inadequate coverage of the area corresponding to the nasal RNFL sector (see Figure 1).

All the participants in this study had reproducible glaucomatous VF defects with corresponding optic disc changes, which may result in overestimation of the structure-function correlation in glaucoma. It would be difficult to avoid this bias because these two criteria are generally regarded as the diagnostic standard of glaucoma in clinical practice. However, we believe our study results should not have been affected much by this potential bias because our purpose was to investigate whether the structure-function association differs between POAG and PACG. We enrolled only patients with high pressure POAG and PACG because we wanted to have the baseline characteristics as comparable as possible between these two groups, except the inherent differences in the anterior chamber angle configuration and ocular biometrics. A recent study, nevertheless, showed that there was no difference in diffuse RNFL thickness or the spatial pattern of RNFL defects between high- and normal- tension glaucoma, as assessed by OCT.[29]

Sihota et al. found optic disc size is smaller in chronic PACG subjects than that in POAG subjects by using OCT.[30] Another study with Heidelberg Retina Tomograph II from the same investing group revealed no significant difference of disc size between chronic PACG and POAG eyes.[31] The disparity in results between prior studies and our study may be attributable to differences of imaging instruments and study populations. Jonas et al. have shown that with refraction within the range of – 8 D to + 4D, the disc area is independent of refraction error.[32] Since the majority of our study subjects have refraction error within this range, it is likely that difference in disc size between POAG and PACG noted in our study is just a chance finding.

This study has several limitations. First, the study is limited by a small sample, which might in part explain the non-significant difference in global structure-function correlation between the PACG and POAG groups. Second, the patients with PACG were older and had larger optic disc diameters as compared to patients with POAG. However, there is no clear evidence in the literature showing that these characteristics would affect the structure-function correlations. Several studies using SLP have shown a negative correlation in average RNFL thickness with increasing age, yet the effect was very small (0.8-1.9 μm per decade).[33, 34] Besides, we subsequently performed subgroup comparisons for patient with similar age from each diagnostic group and demonstrated similar results. Concerning the optic disc diameter, one prior study on 232 normal subjects showed that it was not correlated with the RNFL measurement as assessed by GDx VCC.[35] Despite that the differences in age and optic disc diameters between groups might not strongly affect the structure-function correlation, we still used the multivariate regression analysis to adjust the potential confounding effect of these differences, and the results were consistent before and after adjustment. Finally, all the participants are of Chinese ethnicity and our study results may not be applicable to patients with other ethnic background.

In summary, the present study demonstrates that there are moderate structure-function correlations in both POAG and PACG. Compared to eyes with POAG, fewer RNFL sectors have significant structure-function correlations in eyes with POAG. Our findings suggest

differences in the pathophysiology of optic nerve damage in these two forms of glaucoma, which deserve further investigation.

## Acknowledgments

Funding/Support: Robert Wojciechowski, Joan E. Bailey-Wilson and Ching-Yu Cheng were employees of the US federal government (Inherited Disease Research Branch, National Human Genome Research Institute, National Institutes of Health) when this work was conducted and prepared for publication.

## References

1. Quigley HA, Katz J, Derick RJ, et al. An evaluation of optic disc and nerve fiber layer examinations in monitoring progression of early glaucoma damage. Ophthalmology 1992;99(1):19–28. [PubMed: 1741133]
2. Reus NJ, Lemij HG. The Relationship between Standard Automated Perimetry and GDx VCC Measurements. Invest Ophthalmol Vis Sci 2004;45(3):840–5. [PubMed: 14985299]
3. Schlottmann PG, De Cilla S, Greenfield DS, et al. Relationship between Visual Field Sensitivity and Retinal Nerve Fiber Layer Thickness as Measured by Scanning Laser Polarimetry. Invest Ophthalmol Vis Sci 2004;45(6):1823–9. [PubMed: 15161846]
4. Reus NJ, Lemij HG. Relationships between standard automated perimetry, HRT confocal scanning laser ophthalmoscopy, and GDx VCC scanning laser polarimetry. Invest Ophthalmol Vis Sci 2005;46 (11):4182–8. [PubMed: 16249497]
5. Leung, CKs; Chong, KKL.; Chan, Wm, et al. Comparative Study of Retinal Nerve Fiber Layer Measurement by StratusOCT and GDx VCC, II: Structure/Function Regression Analysis in Glaucoma. Invest Ophthalmol Vis Sci 2005;46(10):3702–11. [PubMed: 16186352]
6. Bowd C, Zangwill LM, Medeiros FA, et al. Structure-Function Relationships Using Confocal Scanning Laser Ophthalmoscopy, Optical Coherence Tomography, and Scanning Laser Polarimetry. Invest Ophthalmol Vis Sci 2006;47(7):2889–95. [PubMed: 16799030]
7. Foster PJ, Buhrmann R, Quigley HA, Johnson GJ. The definition and classification of glaucoma in prevalence surveys. Br J Ophthalmol 2002;86(2):238–42. [PubMed: 11815354]
8. Congdon NG, Quigley HA, Hung PT, et al. Screening techniques for angle-closure glaucoma in rural Taiwan. Acta Ophthalmol Scand 1996;74(2):113–9. [PubMed: 8739673]
9. Salmon JF, Mermoud A, Ivey A, et al. The prevalence of primary angle closure glaucoma and open angle glaucoma in Mamre, western Cape, South Africa. Arch Ophthalmol 1993;111(9):1263–9. [PubMed: 8363470]
10. Gazzard G, Foster PJ, Devereux JG, et al. Intraocular pressure and visual field loss in primary angle closure and primary open angle glaucomas. Br J Ophthalmol 2003;87(6):720–5. [PubMed: 12770969]
11. Gazzard G, Foster PJ, Viswanathan AC, et al. The severity and spatial distribution of visual field defects in primary glaucoma: a comparison of primary open-angle glaucoma and primary angle-closure glaucoma. Arch Ophthalmol 2002;120(12):1636–43. [PubMed: 12470136]
12. Uchida H, Yamamoto T, Tomita G, Kitazawa Y. Peripapillary atrophy in primary angle-closure glaucoma: a comparative study with primary open-angle glaucoma. Am J Ophthalmol 1999;127(2): 121–8. [PubMed: 10030551]
13. Leung CK, Chan WM, Chong KK, et al. Comparative study of retinal nerve fiber layer measurement by StratusOCT and GDx VCC, I: correlation analysis in glaucoma. Invest Ophthalmol Vis Sci 2005;46(9):3214–20. [PubMed: 16123421]
14. Johnson CA, Keltner JL, Cello KE, et al. Baseline visual field characteristics in the ocular hypertension treatment study. Ophthalmology 2002;109(3):432–7. [PubMed: 11874743]
15. Vingrys AJ, Demirel S. False-response monitoring during automated perimetry. Optom Vis Sci 1998;75(7):513–7. [PubMed: 9703040]
16. Newkirk MR, Gardiner SK, Demirel S, Johnson CA. Assessment of false positives with the Humphrey Field Analyzer II perimeter with the SITA Algorithm. Invest Ophthalmol Vis Sci 2006;47(10):4632–7. [PubMed: 17003461]

17. Investigators of AGIS. Advanced Glaucoma Intervention Study 2. Visual field test scoring and reliability. Ophthalmology 1994;101(8):1445–55. [PubMed: 7741836]
18. Garway-Heath DF, Poinoosawmy D, Fitzke FW, Hitchings RA. Mapping the visual field to the optic disc in normal tension glaucoma eyes. Ophthalmology 2000;107(10):1809–15. [PubMed: 11013178]
19. Weinreb RN, Shakiba S, Zangwill L. Scanning laser polarimetry to measure the nerve fiber layer of normal and glaucomatous eyes. Am J Ophthalmol 1995;119(5):627–36. [PubMed: 7733188]
20. Bagga H, Greenfield DS, Feuer WJ. Quantitative assessment of atypical birefringence images using scanning laser polarimetry with variable corneal compensation. Am J Ophthalmol 2005;139(3):437–46. [PubMed: 15767051]
21. Koenker, RaKH. Quantile Regression. Journal of Economic Perspectives 2003;15:143–56.
22. Cheng HM, Singh OS, Kwong KK, et al. Shape of the myopic eye as seen with high-resolution magnetic resonance imaging. Optom Vis Sci 1992;69(9):698–701. [PubMed: 1437010]
23. Atchison DA, Jones CE, Schmid KL, et al. Eye shape in emmetropia and myopia. Invest Ophthalmol Vis Sci 2004;45(10):3380–6. [PubMed: 15452039]
24. Boland MV, Zhang L, Broman AT, et al. Comparison of optic nerve head topography and visual field in eyes with open-angle and angle-closure glaucoma. Ophthalmology 2008;115(2):239–45 e2. [PubMed: 18082888]
25. Huang XR, Knighton RW. Microtubules contribute to the birefringence of the retinal nerve fiber layer. Invest Ophthalmol Vis Sci 2005;46(12):4588–93. [PubMed: 16303953]
26. Mai TA, Reus NJ, Lemij HG. Structure-function relationship is stronger with enhanced corneal compensation than with variable corneal compensation in scanning laser polarimetry. Invest Ophthalmol Vis Sci 2007;48(4):1651–8. [PubMed: 17389496]
27. Huang XR, Bagga H, Greenfield DS, Knighton RW. Variation of peripapillary retinal nerve fiber layer birefringence in normal human subjects. Invest Ophthalmol Vis Sci 2004;45(9):3073–80. [PubMed: 15326123]
28. Cense B, Chen TC, Park BH, et al. Thickness and birefringence of healthy retinal nerve fiber layer tissue measured with polarization-sensitive optical coherence tomography. Invest Ophthalmol Vis Sci 2004;45(8):2606–12. [PubMed: 15277483]
29. Konstantakopoulou E, Reeves BC, Fenerty C, Harper RA. Retinal nerve fiber layer measures in high- and normal-tension glaucoma. Optom Vis Sci 2008;85(7):538–42. [PubMed: 18594346]
30. Sihota R, Sony P, Gupta V, et al. Comparing glaucomatous optic neuropathy in primary open angle and chronic primary angle closure glaucoma eyes by optical coherence tomography. Ophthalmic Physiol Opt 2005;25(5):408–15. [PubMed: 16101946]
31. Sihota R, Saxena R, Taneja N, et al. Topography and fluorescein angiography of the optic nerve head in primary open-angle and chronic primary angle closure glaucoma. Optom Vis Sci 2006;83(7):520–6. [PubMed: 16840877]
32. Jonas JB. Optic disk size correlated with refractive error. Am J Ophthalmol 2005;139(2):346–8. [PubMed: 15734000]
33. Lee VW, Mok KH. Nerve fibre layer measurement of the Hong Kong Chinese population by scanning laser polarimetry. Eye 2000;14(Pt 3A):371–4. [PubMed: 11027003]
34. Da Pozzo S, Iacono P, Marchesan R, et al. The effect of ageing on retinal nerve fibre layer thickness: an evaluation by scanning laser polarimetry with variable corneal compensation. Acta Ophthalmol Scand 2006;84(3):375–9. [PubMed: 16704701]
35. Da Pozzo S, Iacono P, Michelone L, et al. Correlation between optic disc area and retinal nerve fiber layer thickness: a study on scanning laser polarimetry with variable corneal compensation. Graefes Arch Clin Exp Ophthalmol 2007;245(4):511–5. [PubMed: 17111151]

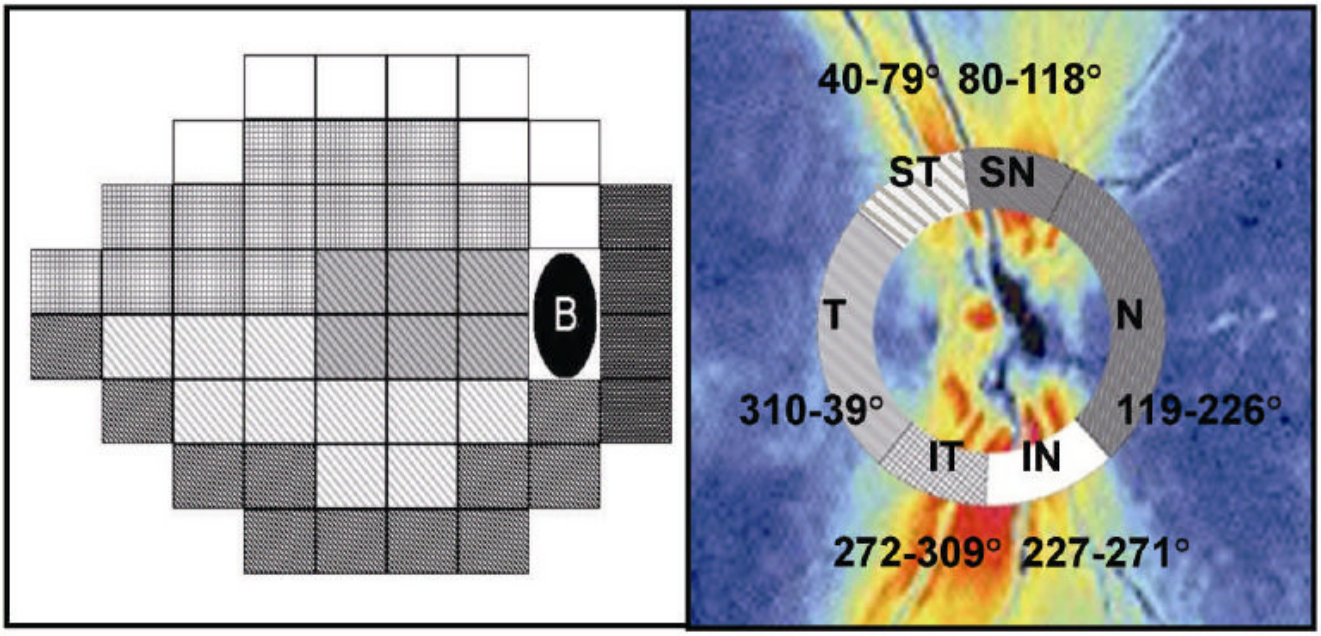


**Figure 1.**
Humphrey Field Analyzer 24-2 test pattern (*left*) and scanning laser polarimetry (GDx VCC) retardation map (*right*) for a right eye. Visual field test points and peripapillary GDx VCC measurements were grouped in six corresponding sectors as defined by Reus et al.[2], which were based on the originally described map by Garway-Heath et al.[18] (T: temporal, ST: superotemporal, SN: superonasal, N: nasal, IN: inferonasal, IT: inferotemporal)

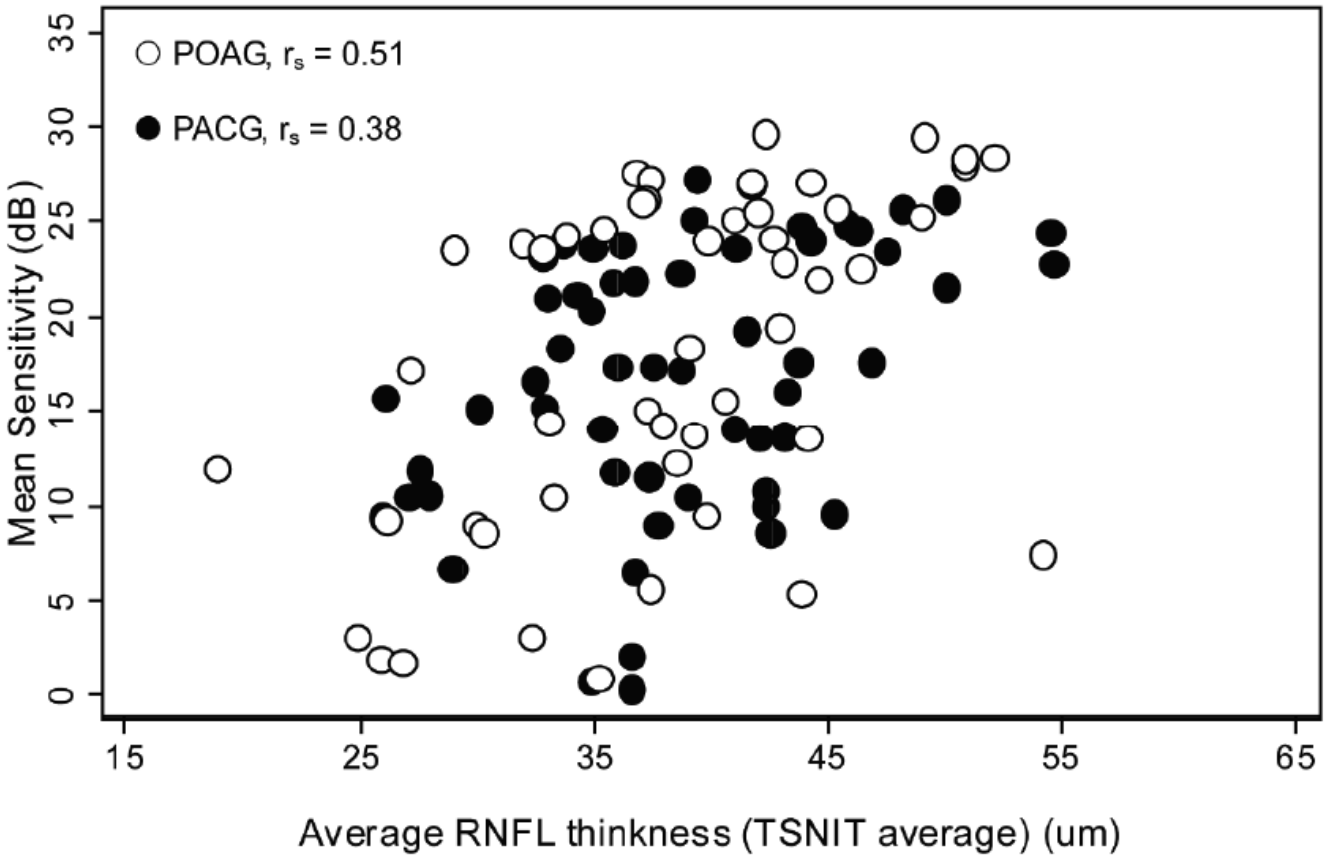


**Figure 2.**
Scatterplots of average peripapillary retinal nerve fiber layer (RNFL) thickness against VF sensitivity expressed in the decibel (dB) scale in POAG eyes and PACG eyes. (○ POAG, ● PACG, TSNIT= temporal-superior-nasal-inferior-temporal, $r_s$ = Spearman's rank correlation coefficient)

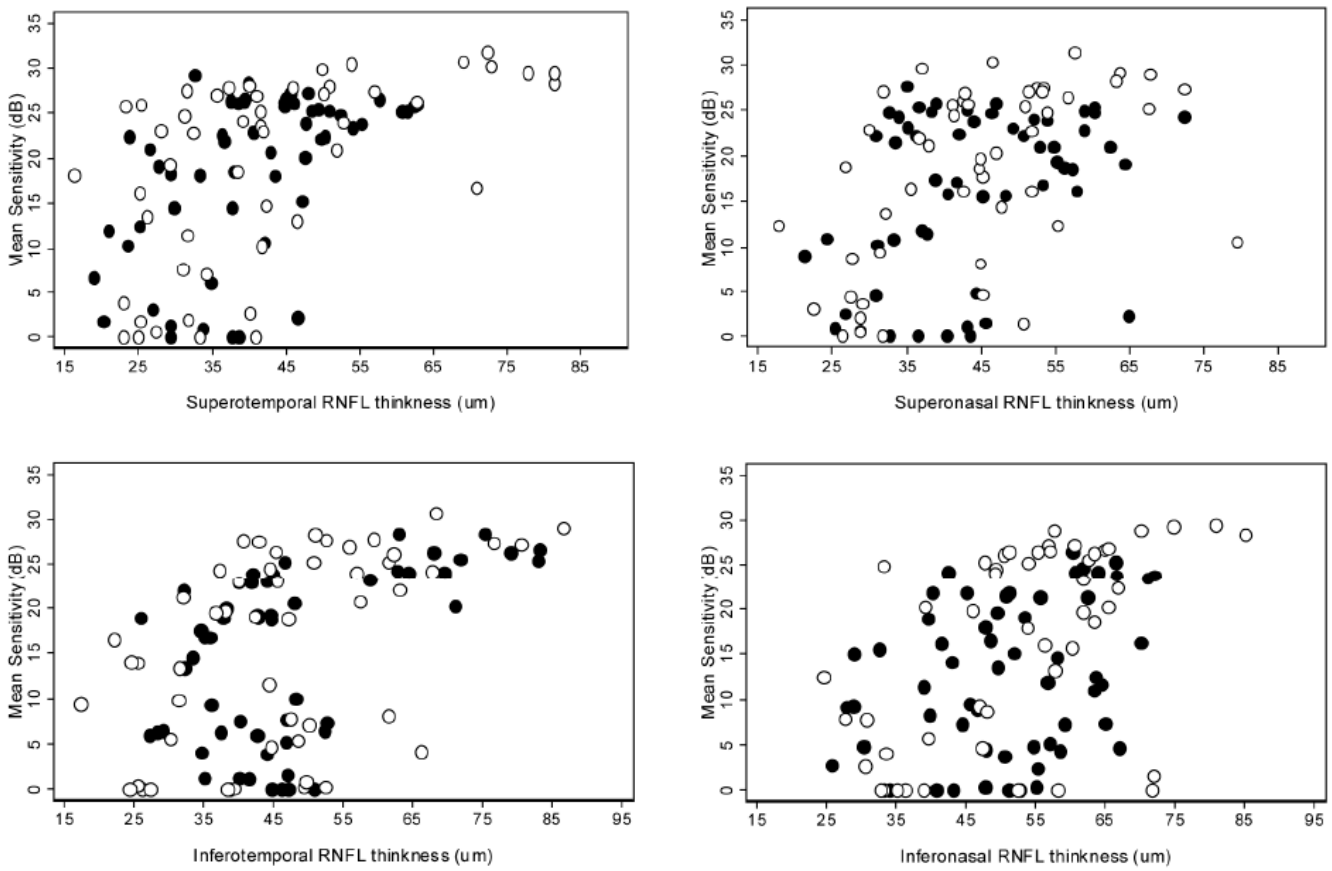


**Figure 3.**

Scatterplots of sectoral peripapillary retinal nerve fiber layer (RNFL) thickness against with VF sensitivity expressed in the decibel (dB) scale in POAG eyes and PACG eyes. (Top left) superotemporal, (Top right) superonasal, (Bottom left) inferotemporal, and (Bottom right) inferonasal sectors. (○ POAG, ● PACG)

## Table 1

Demographic and clinical characteristics of patients

| Characteristics | POAG (*n* = 50) | PACG (*n* = 56) | *P* Value |
|---|---|---|---|
| Age, years | 60.8 ± 17.0 | 71.4 ± 9.5 | <0.001 |
| Gender, female, n (%) | 18 (36) | 25 (45) | 0.366 |
| Right eye, n (%) | 30 (60) | 35 (62.5) | 0.792 |
| Intraocular pressure at enrollment, mmHg | 15.9 ± 4.3 | 14.3 ± 3.4 | 0.032 |
| Spherical equivalent, diopter | -1.70 ± 3.38 | 0.03 ± 1.33 | <0.001 |
| Axial length, mm | 24.38 ± 1.38 | 22.70 ± 0.81 | <0.001 |
| Vertical cup to disc ratio | 0.78 ± 0.12 | 0.78 ± 0.10 | 0.987 |
| Horizontal disc diameter, mm | 1.49 ± 0.29 | 1.63 ± 0.13 | 0.001 |
| Vertical disc diameter, mm | 1.66 ± 0.24 | 1.75 ± 0.16 | 0.027 |
| Visual field mean sensitivity, dB | 18.24 ± 8.90 | 16.82 ± 6.92 | 0.144 |
| Visual field mean sensitivity, 1/L | 367.19 ± 320.47 | 221.48 ± 145.12 | 0.055 |
| Visual field mean deviation, dB | -11.91 ± 9.06 | -12.47 ± 7.48 | 0.357 |
| Visual field pattern standard deviation, dB | 7.15 ± 3.63 | 7.71 ± 3.61 | 0.369 |
| TSNIT average, μm | 38.32 ± 7.71 | 38.64 ± 6.76 | 0.822 |
| TSNIT standard deviation, μm | 13.35 ± 5.13 | 12.31 ± 4.17 | 0.253 |
| NFI | 54.0 ± 21.3 | 49.8 ± 18.5 | 0.284 |

PACG= primary angle closure glaucoma; POAG= primary open angle glaucoma; 1/L= 1/Lambert; TSNIT= temporal-superior-nasal-inferior-temporal; NFI = nerve fiber index

Data are expressed as mean ± standard deviation, except for gender and eye.

**Table 2**

Structure-function correlations between RNFL thickness, measured with GDx VCC, and VF sensitivity, expressed in the decibel (dB) scale in POAG eyes and PACG eyes

| | POAG (*n* = 50) | | | PACG (*n* = 56) | | |
|---|---|---|---|---|---|---|
| **RNFL Thickness** | **$r_s$** | ***P* Value** [c] | **Pseudo $R^2$** [d] | **$r_s$** | ***P* Value** [c] | **Pseudo $R^2$** [d] |
| TSNIT average | 0.51 | <0.001 [e] | 0.31 | 0.38 | 0.004 [e] | 0.17 |
| Superotemporal (ST) | 0.62 | <0.001 [e] | 0.21 | 0.53 | <0.001 [e] | 0.20 |
| Superonasal (SN) | 0.56 | <0.001 [e] | 0.26 | 0.30 | 0.026 | 0.12 |
| Nasal (N) | 0.19 | 0.19 | 0.17 | 0.23 | 0.091 | 0.08 |
| Inferotemporal (IT) | 0.50 | <0.001 [e] | 0.23 | 0.48 | <0.001 [e] | 0.29 |
| Inferonasal (IN) | 0.53 | <0.001 [e] | 0.41 | 0.31 | 0.019 | 0.12 |
| Temporal (T) | 0.23 | 0.111 | 0.11 | 0.05 | 0.703 | 0.09 |

[a] RNFL= retinal nerve fiber layer; GDx VCC= scanning laser polarimetry with variable corneal compensation; VF= visual field; POAG= primary open angle glaucoma; PACG= primary angle-closure glaucoma; TSNIT= temporal-superior-nasal-inferior-temporal

[b] $r_s$ = Spearman's rank correlation coefficient. Data are shown in global average and six corresponding measurement sectors.

[c] *P* value for Spearman's rank correlation coefficient.

[d] Pseudo $R^2$ is from the multivariate median regression model adjusted for age, sex, axial length, and horizontal and vertical disc diameters.

[e] Statistically significance: significance was set at $P < 0.05$ for global correlations and $P < 0.0083$ for each sector as the correction for multiple comparisons.

**Table 3**

Structure-function correlations between RNFL thickness, measured with GDxVCC, and VF sensitivity, expressed in the 1/Lambert (1/L) scale in POAG eyes and PACG eyes

| | POAG (*n* = 50) | | | PACG (*n* = 56) | | |
|---|---|---|---|---|---|---|
| **RNFL Thickness** | **$r_s$** | ***P* Value** [c] | **Pseudo $R^2$** [d] | **$r_s$** | ***P* Value** [c] | **Pseudo $R^2$** [d] |
| TSNIT average | 0.49 | <0.001 [e] | 0.39 | 0.40 | 0.003 [e] | 0.18 |
| Superotemporal (ST) | 0.63 | <0.001 [e] | 0.36 | 0.53 | <0.001 [e] | 0.27 |
| Superonasal (SN) | 0.55 | <0.001 [e] | 0.30 | 0.32 | 0.017 | 0.13 |
| Nasal (N) | 0.18 | 0.199 | 0.27 | 0.20 | 0.140 | 0.07 |
| Inferotemporal (IT) | 0.50 | <0.001 [e] | 0.38 | 0.42 | 0.001 [e] | 0.35 |
| Inferonasal (IN) | 0.52 | <0.001 [e] | 0.40 | 0.31 | 0.020 | 0.06 |
| Temporal (T) | 0.21 | 0.150 | 0.25 | 0.14 | 0.311 | 0.11 |

[a] RNFL= retinal nerve fiber layer; GDx VCC= scanning laser polarimetry with variable corneal compensation; VF= visual field; 1/L = 1/Lambert; POAG= primary open angle glaucoma; PACG= primary angle-closure glaucoma; TSNIT= temporal-superior-nasal-inferior-temporal

[b] $r_s$ = Spearman's rank correlation coefficient. Data are shown in global average and six corresponding measurement sectors.

[c] *P* value for Spearman's rank correlation coefficient.

[d] Pseudo $R^2$ is from the multivariate median regression model adjusted for age, sex, axial length, and horizontal and vertical disc diameters.

[e] Statistically significance: significance was set at $P < 0.05$ for global correlations and $P < 0.0083$ for each sector as the correction for multiple comparisons.